ACS Macro Letters

Letter

pubs.acs.org/macroletters

A Combined Strategy to Surface-Graft Stimuli-Responsive Hydrogels Using Plasma Activation and Supercritical Carbon Dioxide

Telma Barroso,[†] Raquel Viveiros,[†] Márcio Temtem,[†,§] Teresa Casimiro,[†] Ana M. Botelho do Rego,[‡] and Ana Aguiar-Ricardo*[,†]

[†]REQUIMTE, Departamento de Química, Faculdade de Ciências e Tecnologia, Universidade Nova de Lisboa, 2829-516 Caparica, Portugal

[‡]Centro de Química-Física Molecular (CQFM) and Institute of Nanoscience and Nanotechnology (IN), Departamento de Engenharia Química, Instituto Superior Técnico, Universidade Técnica de Lisboa, Lisboa, Portugal

Supporting Information

ABSTRACT: Differently shaped polymeric matrices were efficiently coated with stimuli-responsive hydrogels for a wide range of applications using a new methodology. By combining plasma surface activation and polymerization in supercritical media at mild conditions, we report the direct smart coating of microcarriers and membranes in gram-scale quantities with a scalable, green, and low-cost approach.

The ability to prepare "smart" coatings by surface-grafting polymeric hydrogels is playing an increasingly important part in a diverse range of applications, such as drug delivery,[1] diagnostics,[2] and tissue engineering,[3] as well as biosensors[4] or microelectromechanical systems.[5] There is a need for absolute control over the hydrogel layer morphology covering a range of devices, including those with large area sizes, nonplanar geometries, and porous or nonporous surfaces.[6] Herein, we describe the use of a new green methodology based on the combination of plasma surface activation and supercritical carbon dioxide ($scCO_2$) assisted polymerization to prepare "smart" switchable polymeric microparticles and membranes. By using this new approach, we show that an effective stimuli responsive coating of polymeric matrices can be achieved at mild conditions without using hazardous organic solvents, stabilizers or radical initiators. The developed procedure consists in two main steps: (i) the formation of radicals along the surface of a material by plasma treatment (e.g., argon plasma treatment) followed by (ii) graft-polymerization of a stimuli sensitive polymer in supercritical carbon dioxide ($scCO_2$). Following this procedure, we prepared differently shaped temperature-responsive devices: (i) active microcarriers and (ii) hydrogel composite membranes.

Microcarriers are used to expand anchorage dependent cells in large-scale suspension bioreactors. A common procedure to detach cultured cells uses proteolytic enzyme treatment, for example, trypsin or collagenase; harvesting cells from the carriers is difficult, inevitably damages extracellular proteins, and can even alter the structure and function of cell surface. To overcome these drawbacks, coating microcarriers with a thermoresponsive polymer has been suggested as a suitable alternative method.[7] The strong polymer conformational changes induced by a decrease of temperature can be used for cell harvesting without enzymatic or mechanical treatment. The most studied thermoresponsive polymer is poly(*N*-isopropylacrylamide) (PNIPAAm) characterized by the so-called lower critical solution temperature (LCST). Around 31−32 °C the microgel undergoes a volume phase transition from a swollen to a collapsed state in aqueous solution. At temperatures above the LCST, intramolecular H-bonding between amide groups and increasing hydrophobic interactions among isopropyl groups prevails, leading to a compact conformation of PNIPAAm.[8−10] These structural changes may be used to free the cell from their carrier for subsequent collection and/or replating.[11] Cytopore 2 (CYT2) and cytodex 3 (CYT3) are examples of frequently used microbead systems to expand anchorage-dependent cells in culture;[12] hence the effort to improve coating strategies that allow the regulation of its hydrophilic/hydrophobic behavior by small temperature changes is fully justified.

Stimuli-responsive membranes that combine a rigid porous membrane with a responsive hydrogel layer are of great interest for mass separation, sensing and analytics, (bio)catalysis, biomedical engineering, and microsystem technologies.[2,13,14] Many of these applications require hydrogels as thin layers at surfaces. The interplay of the membrane pore structure, its composition, and the structural diversity of the hydrogels can lead to different advanced composite membranes. One surface-selective approach successfully employed for membrane surface functionalization with hydrogels consists of the "grafting from"

Received: October 31, 2011
Accepted: February 6, 2012
Published: February 14, 2012

technique.[15] This heterogeneous technique is a surface-initiated polymerization process whereby polymer chains grow from initiator sites on the membrane surface by monomer addition from the solution method. One simple way to introduce the initiator sites onto the membrane outer surface is to irradiate the membrane with argon plasma to form initiator radicals. In conventional "grafting from" techniques the polymerization is then carried out from these initiator sites by immersing the treated membranes in monomer solutions. At the end, several washes with organic solvents are performed to eliminate all of the possible vestiges of monomer retained in activated materials. The separation performance of the resulting membrane is clearly controlled by the hydrogel and the way it is incorporated into the base membrane. One example is the different resulting performance of PNIPAAm and poly(*N*,*N*′-diethylacrylamide) (PDEAAm) coatings on polysulfone-based membranes when using $scCO_2$ technology to perform the in situ polymerization. The hydrogel coating layers were able to minimize membranes fouling behavior, but the resulting performances of both coatings in protein separation processes were differently dependent on the base membrane blend composition.[16,17] While PNIPAAm coatings on polysulfone (PS) and polyacrylonitrile (PAN) blended matrices (represented as PS/PAN membranes hereafter) do not endow a temperature-responsive behavior to the membrane surface, PDEAAm coatings on the same membranes were revealed to confer temperature-dependent permeabilities and showed selective permeation of proteins with different sizes. In this previous work the hydrogel synthesis was induced by a radical initiator, and the polymeric hydrogel network was physically adsorbed onto the membrane surface with poor control of the uniformity and thickness of the hydrogel coating layer. Herein we developed a PS/PAN blended membrane grafted with PDEAAm using for the first time a nonwet green methodology by combining plasma surface activation and supercritical fluid technology. The surface activation by plasma treatment induces the formation of active sites (radicals) from which DEAAm polymerization can initiate and uniformly cover the membrane surface with a continuously synthetic hydrogel layer. The resulting thermoresponsive membrane is obtained pure, sterile, and ready-to-use without further purification steps.

Following the suggested new strategy, controlled hydrogel coating layers can be designed on top of polymeric devices of any geometry as demonstrated as a proof of concept for microcarriers CYT2 and CYT3 and for PS/PAN blended membranes. The in situ polymerization of NIPAAm over CYT2 and CYT3 and of DEAAm within the PS/PAN membrane pores was performed by loading the native samples activated by Ar plasma treatment into the high-pressure cell with weighted monomers in the bottom of the cell. For easier manipulation of samples during plasma activation and $scCO_2$ polymerization steps, CYT2 and CYT3 were processed to form films with tailored size and shape by compression molding (Figure S1A, in the Supporting Information). The polymerization followed the normal general procedures as described in detail in our previous works, but with the following modifications: (i) the hydrogel was synthesized at 37 °C and 20 MPa to ensure high $scCO_2$ density, and as surface materials were previously activated by plasma treatment no radical thermal initiation was needed; (ii) all of the equipment was manipulated in a fume-board with controlled inert atmosphere to minimize side reactions with oxygen and the formation of peroxides, while the activated devices are transferred from the plasma chamber to the high-pressure cell (Supporting Information, Figure S1). PNIPAAm and PDEAAm were synthesized without a cross-linker to maximize its temperature responsiveness.[9] At the end of the reactions, the resulting thermoresponsive devices were slowly washed with fresh high-pressure CO_2 to clean the remaining residues of unreacted monomer and render the materials with high purity. The PS/PAN membranes were prepared using the $scCO_2$ induced phase inversion method following the procedure described in detail by Temtem et al.[17]

Scanning electron microscopy (SEM) revealed the formation of PNIPAAm coatings completely covering the microcarriers (Figure 1A–D) as well as the top surface of PS/PAN membrane samples with a PDEAAm film (Figure 1E,F). We investigated the microstructure of CYT2, CYT3, and PS/PAN membrane samples before and after the coating procedure using the novel methodology to coat the surfaces with two different hydrogels PNIPAAm that is a more compliant hydrogel and PDEAAm that is a stiffer one.[16]

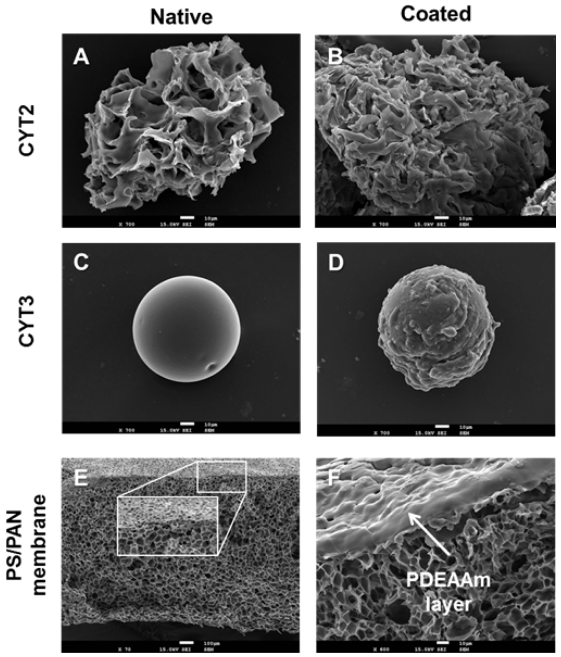

Figure 1. Scanning electron micrographs of the microcarriers and the membrane before and after the hydrogel coating: (A) native CYT2; (B) PNIPAAm-coated CYT2; (C) native CYT3; (D) PNIPAAm-coated CYT3; (E) native PS/PAN membrane with a magnified region showing the micropores on the membrane top surface; (F) coated PS/PAN membrane showing a dense PDEAAm layer obstructing the pores on the top surface.

The microcarriers were coated with PNIPAAm as no toxic effect over fibroblast cell cultures was observed, and this hydrogel can be manipulated in agreement with the mechanical behavior of a target tissue to promote a physiological sustainable interaction between the material and surrounding cells.[10] PDEAAm was the selected hydrogel to confer temperature responsiveness to PS/PAN blended membranes as it was previously demonstrated that PNIPAAm coatings on PS/PAN matrices does not endow a temperature-responsive behavior to the membrane surface due to the more favorable interaction between PNIPAAm chains and PS/PAN membrane surface which hampers the PNIPAAm chains stretching conformations and the hydrogen-bond interactions of the

dx.doi.org/10.1021/mz200145w | *ACS Macro Lett.* 2012, 1, 356–360

amide groups.[16] The PNIPAAm covering CYT2 and CYT3 appears as a thin and dense layer over the irregular structure of CYT2 and over the spherical ball of CYT3. Finally, the PS/PAN coated membrane presents a compact PDEAAm layer partially obstructing the pores on the top surface (Figure 2F).

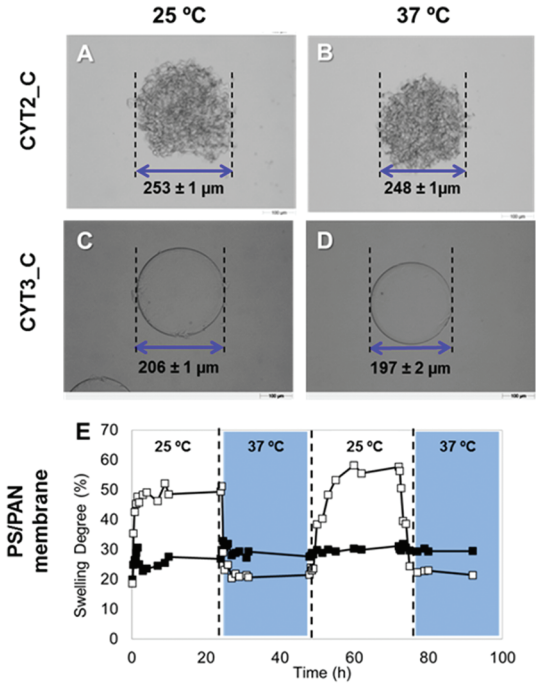

Figure 2. Optical micrographs for hydrated PNIPAAm-coated CYT2 at 25 °C (A) and 37 °C (B) and for coated CYT3 at 25 °C (C) and at 37 °C (D), in phosphate buffer solution at pH 7.4. The small dimensional change of microcarrier average diameter is due to the collapse of the thin PNIPAAm outer layer upon temperature increase. (E) Reversible swelling behavior of PS/PAN membrane at 25 and 37 °C: (□) coated with PDEAAm and (■) native.

The thickness of membranes was estimated from full cross section SEM micrographs. The membrane thickness increased from 1.13 ± 0.02 mm (native membrane) to 1.17 ± 0.02 mm for coated membranes. The extent of surface coating was also evaluated through swelling measurements at 25 and 37 °C (below and above the LCST of PNIPAAm and PDEAAm). Optical micrographs of the CYT2 and CYT3 dispersed in 10 mM phosphate buffer solutions are shown in Figure 2A–D for 25 and 37 °C, revealing a slight decrease in average size diameter with increasing temperature (further experimental details in Supporting Information). The swelling experiments also demonstrate that the coated membrane change reversibly its water uptake capacity, 50 to 20%, when the environmental temperature is altered from 25 to 37 °C, while the native membrane presents a constant swelling degree (Figure 2E).

Recognizing the importance of screening hydrophilicity behavior as a function of temperature, we measured water contact angles on PS/PAN membranes and on films made from coated and native CYT2 and CYT3. Water contact angles for coated CYT3 clearly revealed the change from an hydrophilic surface with a contact angle of 43° at 25 °C to an hydrophobic surface with a contact angle of 104° at 37 °C. As CYT2 presents a superporous structure, it was not possible to measure the contact angles using the drop shape method. The native membrane showed a rather constant water contact angle around 80°, while the PDEAAm coated membrane changed the water contact angle from 41° to 74° by increasing the temperature from 25 to 37 °C. These temperature-dependent contact angle values ensure the efficiency of the methodology followed on grafting PDEAAm onto the membrane surface.

Next, we employed X-ray photoelectron spectroscopy (XPS) to examine the elemental compositions of the outer surfaces of CYT2, CYT3, and PS/PAN membrane samples before and after coating with PNIPAAm and PDEAAm, respectively (Figure 3). XPS was previously used to show that PS/PAN

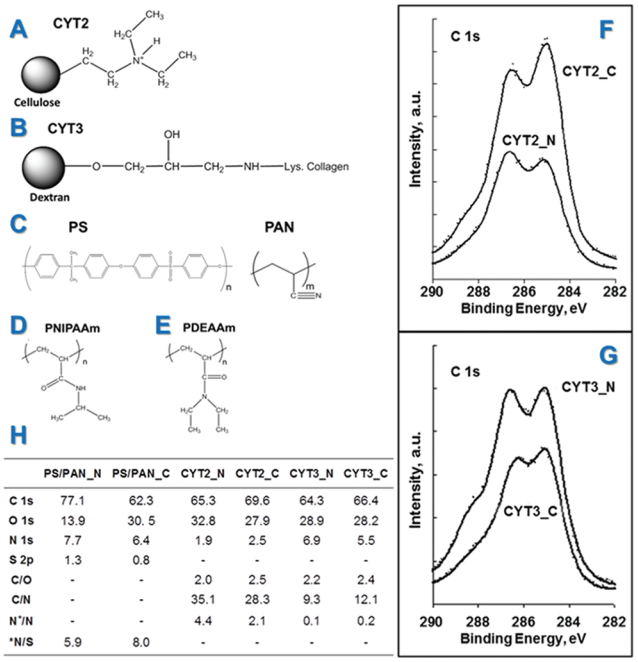

H

	PS/PAN_N	PS/PAN_C	CYT2_N	CYT2_C	CYT3_N	CYT3_C
C 1s	77.1	62.3	65.3	69.6	64.3	66.4
O 1s	13.9	30. 5	32.8	27.9	28.9	28.2
N 1s	7.7	6.4	1.9	2.5	6.9	5.5
S 2p	1.3	0.8	-	-	-	-
C/O	-	-	2.0	2.5	2.2	2.4
C/N	-	-	35.1	28.3	9.3	12.1
N°/N	-	-	4.4	2.1	0.1	0.2
°N/S	5.9	8.0	-	-	-	-

Figure 3. Chemical compositions of different materials: (A) CYT2; (B) CYT3; (C) polymers blended in the membrane; (D) PNIPAAm; and (E) PDEAAm. XPS spectrum of native and coated microcarriers: carbon (C 1s) peak for CYT2 (F) and CYT3 (G). (H) Elemental surface composition of native and coated CYT2, CYT3, and PS/PAN membranes.

membrane could be successfully coated with PNIPAAm and PDEAAm by $scCO_2$-assisted polymerization using azobisisobutyronitrile (AIBN) as the inititiator,[16] but in this study we have proven that the grafting-from using $scCO_2$ media after matrix Ar plasma treatment can lead to the formation of a continuous coverage of the surface with the in situ synthesized polymer. C 1s, O 1s, and N 1s regions were studied for all of the samples, and the S 2p region study stands only for the membrane. The global atomic % is gathered in Figure 3H. The ratio N/S is a good parameter to assess the effectiveness of the coating, as only the membrane contains sulfur, while nitrogen is present in both the membrane and the coating. In fact, the N/S atomic ratio increases from 5.9 to 8 which means that the signal of S 2p photoelectrons was attenuated after coating.

A large increase of oxygen was also observed for PS/PAN coated membranes, and this fact may be due to some CO_2 occlusion inside the coating itself. Already in the uncoated membrane, an amount of oxygen larger than expected was found (experimentally, O/S~10 whereas O/S = 4 was stoichiometrically expected) which may have the same cause. The presence of water, as a possible cause for the excess of oxygen, was discarded since the O 1s region does not present

dx.doi.org/10.1021/mz200145w | ACS Macro Lett. 2012, 1, 356–360

any components for BE > 533.5 eV. Quantitative data also attests that the coating of the microcarriers was achieved since: (i) CYT2 sample, under the native form, has a large content of oxygen (C/O = 1.2 for cellulose) except in the extreme surface where a branched chain containing six carbons and an ionized nitrogen is grafted. Since PNIPAAm has atomic ratios of C/O = C/N = 6 and a large proportion of aliphatic carbon (sp^3 carbons bound to C and/or H) is typically found at a binding energy of 285 eV, both the atomic ratio C/O and the relative magnitude of the aliphatic peak in the C 1s region are expected to increase upon the successful coating with PNIPAAm, as confirmed by data shown in Figure 3H. Also the relative amount of nitrogen, specially in the nonionized form (N from PNIPAAm) should increase since the PNIPAAm puts one additional N for each additional six carbons but covers the ionized nitrogens of the external layer. Values from XPS analysis confirm both hypotheses; (ii) CYT3, in its native form, besides the polysaccharide in the nucleus, exhibits a shell composed of a complex mixture of amino-acids having a large relative amount of nitrogen (with C/N ≪ 6), much larger than in CYT2, whereas the relative amount of oxygen is a bit smaller than for CYT2 since the outer shell is certainly thick enough to attenuate the contribution of the polysaccharide. Here the coating with PNIPAAm is also attested by the relative amount of aliphatic carbon (Figure 3G), an increase of atomic C/O (more modest than in CYT2), and contrarily to the CYT2 case, a decrease of the relative amount of nitrogen. This is due to the fact that the atomic ratio C/N is larger in PNIPAAm than in collagen. The intriguing value is the ratio N^+/N which increases with the coating. Since in this sample the ionized nitrogen must originate from zwitterionic forms of the aminoacids (like glycine, for instance), it may happen that the bead activation by the plasma and/or the interaction with the PNIPAAm favors the zwitterionic formation. No further XPS data exploration is possible, namely, angular studies, given the large surface roughness which avoids any quantitative estimation of coating thickness and/or substrate coverage degree.

Finally, to evaluate the thermoresponsive efficacy of the grafted-PDEAAm coating on controlling permeability and interactions with biomolecules, we permeated pure water and buffered solutions of bovine serum albumin (BSA), a model protein, at different temperatures. As expected, the water permeability of these membranes showed temperature sensitivity, showing a 2-fold increase when temperature changed from 25 to 37 °C, but the permeability for the unmodified membranes did not significantly change (data in Figure 4A).

For the standard filtration assays, coated PS/PAN membrane was equilibrated by eluting 10 mL of phosphate buffer solution (PBS); then feed BSA solution (3 mg mL^{-1}) was filtrated at pH 7.4 (loading step), and finally a last PBS wash was performed, to recover the BSA retained (washing step). The different BSA filtration profiles, obtained at 25 and 37 °C, are plotted in Figure 4B. At 37 °C higher BSA permeation occurs (90%) than at 25 °C (43%) due to the more hydrophobic character of PDEAAm chains at 37 °C. At 25 °C, the membrane surface is more hydrophilic; the expanded PDEAAm chains block the pores and consequently hinder the permeation. It is clear that the washing step efficiently eluted out the adsorbed BSA from the grafted membrane as no irreversible fouling was observed. This thermodynamically driven hydrophilic−hydrophobic behavior of PDEAAm coating near the LCST (~33 °C) can

A

	Porosity (%)	Young Modulus (MPa)	Permeability L/(m².h.MPa)	
			25 °C	37 °C
PS/PAN_N	49	0.58	1150	1164
PS/PAN_C	51	0.54	1369	2866

B

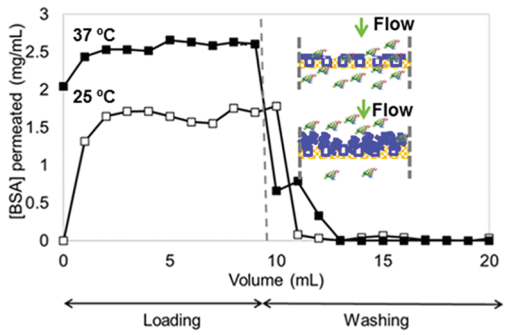

Figure 4. (A) Porosity and the Young modulus of native and coated dry PS/PAN membranes, which are similar. The water permeability coefficient of the PDEAAm-coated membrane doubled at 37 °C compared to that of 25 °C. (B) BSA permeation profiles through PDEAAm coated PS/PAN membrane at 37 °C (■) and 25 °C (□). An inset scheme shows the PDEAAm-grafted temperature-responsive behavior: at 25 °C, PDEAAm brushes are extended and create a hydrophilic physical barrier preventing the BSA permeation; contrarily, at 37 °C, PDEAAm brushes switch to a collapsed structure, and the membrane pores enlarge, facilitating protein permeation.

be explored to generate one-step bioseparation processes based on a cyclical operation of heating and cooling.

We have demonstrated an effective nonwet grafting polymerization route for forming polymeric coatings on porous and nonporous materials with different shapes. Moreover the process could be applied for coating surfaces made from synthetic and natural polymers. We envisage that a change in the conditions, during the plasma treatment and the polymerization reactions in supercritical media, will easily improve the performance of the coating procedure. Also, further studies are required to assess the dependence of polymeric coating thickness and graft density with the chemistry of the base matrices and the monomer equilibrium solubility in $scCO_2$. Depending on the stimuli-sensitive polymer nature, different coverage morphological characteristics can be obtained in terms of the coat thickness and uniformity. It can be anticipated that this green and straightforward coating process can be extended for different base materials as well as diverse polymeric coatings and will find many applications in areas such as stimuli-sensitive microfluidic devices, programmed drug delivery platforms, regenerative medicine, and biotechnology.

■ ASSOCIATED CONTENT

Ⓢ Supporting Information

Information regarding materials, experimental procedures, morphological characterization, and details concerning the filtration assays. This material is available free of charge via the Internet at http://pubs.acs.org.

■ AUTHOR INFORMATION

Corresponding Author

*Tel.: + 351 212949648. E-mail: air@fct.unl.pt.

Present Address
[§]Present address: Hovione, Sete Casas, 2674-506 Loures, Portugal.

Notes
The authors declare no competing financial interest.

■ ACKNOWLEDGMENTS

This project was funded in part by the MIT-Portugal Program and Fundação Calouste Gulbenkian (Plasma equipment) and Fundação para a Ciência e Tecnologia through contracts SFRH/BD/62475/2009 (T.B.), MIT-Pt/BS-CTRM/0051/2008, and POCTI/EQU/116097/2006, FEDER, FSE, and POCTI. A.A.R. acknowledges C. Lobato da Silva for kindly providing the cytopore 2 and cytodex 3 microcarriers.

■ REFERENCES

(1) (a) Alexander, C. *Nat. Mater.* **2008**, *7*, 767−768. (b) Bajpai, A. K.; Shukla, S. K.; Bhanu, S.; Kankane, S. *Prog. Polym. Sci.* **2008**, *33*, 1088−1118. (c) Shi, J.; Votruba, A. R.; Farokhzad, O. C.; Langer, R. *Nano Lett.* **2010**, *10*, 3223−3230.
(2) Roy, D.; Cambre, J. N.; Sumerlin, B. S. *Prog. Polym. Sci.* **2010**, *35*, 278−301.
(3) Ushida, A. K.; Sakai, K.; Ito, E.; Kwon, O. H.; Kikuchi, A.; Yamato, M.; Okano, T. *Biomaterials* **2000**, *21*, 923−929.
(4) Liu, J. *Soft Matter* **2011**, *7*, 6757.
(5) Nash, M. A.; Yager, P.; Hoffman, A. S.; Stayton, O. S. *Bioconjugate Chem.* **2010**, *21*, 2197−2204.
(6) (a) Tokarev, B. I.; Minko, S. *Adv. Mater.* **2010**, *22*, 3446−3462. (b) Stuart, M. A. C.; Huck, W. T. S.; Genzer, J.; Müller, M.; Ober, C.; Stamm, M.; Sukhorukov, G. B.; Szleifer, I.; Tsukruk, V. V.; Urban, M.; Winnik, F.; Zauscher, S.; Luzinov, I.; Minko, S. *Nat. Mater.* **2010**, *9*, 101−113.
(7) Yang, H. S.; Jeon, O.; Bhang, S. H.; Lee, S.-H.; Kim, B.-S. *Cell Transplant.* **2010**, *19*, 1123−1132.
(8) Heskins, M.; Guillet, J. R. *J. Macromol. Sci.* **1968**, *2*, 1441−1455. Pelton, R. H.; Chibante, P. *Colloids Surf.* **1986**, *20*, 247−256.
(9) Temtem, M.; Casimiro, T.; Mano, J. F.; Aguiar-Ricardo, A. *Green Chem.* **2007**, *9*, 75−79.
(10) Costa, E.; Coelho, M.; Ilharco, L. M.; Aguiar-Ricardo, A.; Hammond, P. T. *J. Supercrit. Fluids* **2011**, *56*, 292−298.
(11) (a) Cheng, C.-J.; Chu, L.-Y.; Ren, P.-W.; Zhang, J.; Hu, L. J. *Colloid Interface Sci.* **2007**, *313*, 383−388. (b) Hendrick, V.; Muniz, E.; Geuskens, G.; Werenne. *J. Cytotechnol.* **2001**, *36*, 49−53.
(12) (a) Chen, A. K.-L.; Chen, X.; Choo, A. B. H.; Reuveny, S.; Oh, S. K. W. *Stem Cell Res.* **2011**, *7*, 97−111. (b) Nie, Y.; Bergendahl, V. D. J.; Hei, J. M.; Jones, S. M.; Palecek, P. *Biotechnol. Prog.* **2009**, *25*, 20−31.
(13) Yang, Q.; Adrus, N.; Tomicki, F.; Ulbricht, M. *J. Mater. Chem.* **2011**, *21*, 2783−2811.
(14) Cole, M. A.; Voelcker, N. H.; Thissen, H.; Griesser, H. J. *Biomaterials* **2009**, *30*, 1827−1850.
(15) Wandera, D.; Wickramasinghe, S. R.; Husson, S. M. *J. Membr. Sci.* **2010**, *357*, 6−35.
(16) Barroso, T.; Viveiros, R.; Coelho, M.; Casimiro, T.; Botelho do Rego, A. M.; Aguiar Ricardo, A. *Polym. Adv. Technol.* **2011**, DOI: DOI: 10.1002/pat.2057.
(17) Temtem, M.; Pompeu, D.; Barroso, T.; Fernandes, J.; Simões, P. C.; Casimiro, T.; Botelho do Rego, A. M.; Aguiar-Ricardo, A. *Green Chem.* **2009**, *11*, 638−645.